Green Chemistry

PAPER

View Article Online
View Journal | View Issue

Cite this: *Green Chem.*, 2024, **26**, 7258

Sustainable aviation fuel from prehydrolysis liquors†

Daria Lebedeva,[a] Lars William Schick,[a] Daniel Cracco,[a] Withsakorn Sangsuwan,[a] Gonzalo Castiella-Ona,[a] Dagoberto O. Silva,[c] Alessandro Marson,[d] Erik Svensson Grape,[b] A. Ken Inge, *[b] Liane M. Rossi, *[c] Elena Subbotina,*[a] Alessandro Manzardo*[d] and Joseph S. M. Samec *[a]

Maximizing products of high value and minimizing incineration of side-streams is key to realize future biorefineries. In current textile production from forestry, hemicellulose is removed by prehydrolysis before delignification. The resulting prehydrolysis liquor is incinerated in the recovery boiler at low efficiency. This additional burden on the limiting recovery boiler reduces the pulp production. In this study, we demonstrate that prehydrolysis liquor can be upgraded, in 5 steps, to yield aviation fuels. Prehydrolysis liquors were dehydrated to furfural by zeolite catalysis. Furfural was selectively reduced to furfuryl alcohol by Au@NC. Rhenium-catalysed Achmatowicz rearrangement gave a C_5 intermediate susceptible to self [2 + 2] cycloaddition to give the C_{10} oxygenated precursor. By using a combination of Ru/C and zeolites, full hydrodeoxygenation was achieved. The overall transformation from furfural to hydrocarbons resulted in a 48% carbon yield. The resulting hydrocarbons, containing an anticipated strained four-membered ring, are preferred aviation fuel components. This is an important step to show that aviation fuels can be produced sustainably from existing industrial side-streams. A comparative life cycle assessment was applied to evaluate the environmental impact of the proposed valorization approach, demonstrating benefits in the climate change impact category when implementing this technology in a pulp mill compared to the incineration of pre-hydrolysis liquor scenario.

Received 13th March 2024,
Accepted 20th May 2024

DOI: 10.1039/d4gc01257g

rsc.li/greenchem

Introduction

The increasing demand for sustainable aviation fuel (SAF) is driven by the depletion of fossil resources, awareness of carbon dioxide emissions, and political instability. Due to the extreme demands for propulsion in aviation, shifting towards electric engines is more challenging than for road transportation.[1] For this reason, aviation will require liquid hydrocarbon fuels even in the future. SAF, by definition, requires the utilization of non-fossil-based feedstock; biogenic carbon sources (biomass) or CO_2 are preferred.[2] Currently, SAF:s are made from crops, which is not considered sustainable since this feedstock adversely affects land use and water scarcity. As follows, raw materials sourced from low value streams or wastes are preferred to avoid burdens on climate change and land use.[3]

The generation of prehydrolysis liquor, from hemicelluloses, is a crucial wood pre-treatment step in the dissolving grade pulp production of the kraft process. Dissolving grade pulp is used for generation of textile fibers to substitute cotton production, which has lately been questioned for environmental concerns. The prehydrolysis liquor produced in this process, together with lignin, is currently incinerated to generate heat and power, however at low efficiencies. This brings an additional burden on the rate limiting recovery boiler, reducing the overall production capacity of pulp.[4] Thus, there is a potential to simultaneously increase the value of prehydrolysis liquor beyond its heating value, and debottleneck pulp production (Fig. 1).

The state-of-the-art synthetic pathways for SAF:s includes pioneering research by Dumesic and co-workers, demonstrating the approach for utilizing sugars, such as glucose, to synthesise linear hydrocarbons within aviation boiling point

[a]*Stockholm University, Department of Organic Chemistry, Svante Arrhenius väg 16C, SE 106 91 Stockholm, Sweden. E-mail: joseph.samec@su.se*
[b]*Department of Materials and Environmental Chemistry, Stockholm University, Stockholm SE 10691, Sweden*
[c]*Departamento de Química Fundamental, Instituto de Química, Universidade de São Paulo, Av. Prof. Lineu Prestes, 748, 05508-000, São Paulo, SP, Brazil*
[d]*CESQA (Quality and Environmental Research Center), University of Padova, Department of Civil, Environmental and Architectural Engineering, Via Marzolo 9, 35131 Padova, Italy*

†Electronic supplementary information (ESI) available. CCDC 2307840, 2307841 and 2308513. For ESI and crystallographic data in CIF or other electronic format see DOI: https://doi.org/10.1039/d4gc01257g

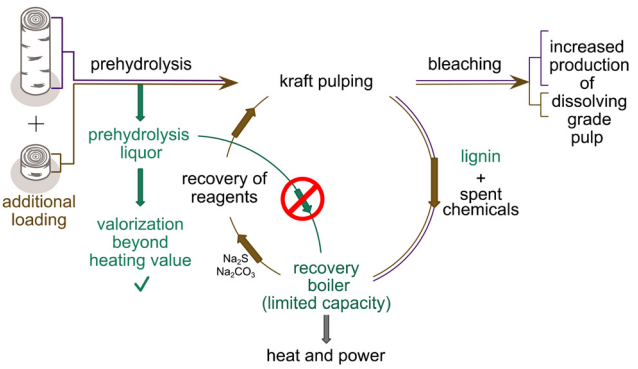

Fig. 1 Increasing the pulp production by emptying the recovery boiler.

range.[5] Another approach was described by Corma and co-workers, who converted sugar-derived furanics into branched alkanes (Scheme 1, entries 1 and 2).[6] Recent advancements have underscored the advantages of cyclic hydrocarbons in fuel applications, owing to their increased energy density and higher heat of combustion. The work by Li's research group demonstrated the synthesis of multicyclic hydrocarbons containing 5-membered rings from cellulose (Scheme 1, entry 3).[7] Nevertheless, it's worth mentioning that cyclobutane's relative strain energy of 26.5 kcal mol^{-1} is notable when compared to cyclopentane (6.2 kcal mol^{-1}) and cyclohexane (0 kcal mol^{-1}).[8] Thus, cyclobutane derivatives could be desired candidates for aviation fuel, as they afford a higher heat of combustion. Several research groups proposed synthetic pathways for preparing cyclobutane-based hydrocarbons from sources that are not as available as the sugars, *vide supra*. These approaches include a [2 + 2] cycloaddition to yield cyclobutane-derivatives from acetone derived isopherone followed by hydrodeoxygenation (HDO), when applicable (Scheme 1, entry 4).[9–12] However, no reports disclose high energy 4-membered SAF:s produced from available side-streams of low value.

In this work, we report a novel value chain from industrially relevant prehydrolysis liquor to produce cyclobutane-containing hydrocarbons suitable for aviation fuel *via* furfural (Scheme 1, entry 5). Our approach involves the multi-step transformation of furfural into C_5 precursors **3** and **4**, susceptible to [2 + 2] cycloaddition, resulting in the formation of cyclobutane **5**, that was successfully hydrotreated to produce high energy C_{10} SAF:s. To ascertain the sustainability of the novel route, a comparative LCA has been performed showing significant reduction in climate change, compared to conventional aviation fuels.

Experimental

General considerations

All chemicals were purchased from Sigma Aldrich, if not stated otherwise. Zeolites were purchased from Zeolyst. Furfural was distilled prior to use. The light-driven reactions were performed using a Rayonet reactor equipped with eight high

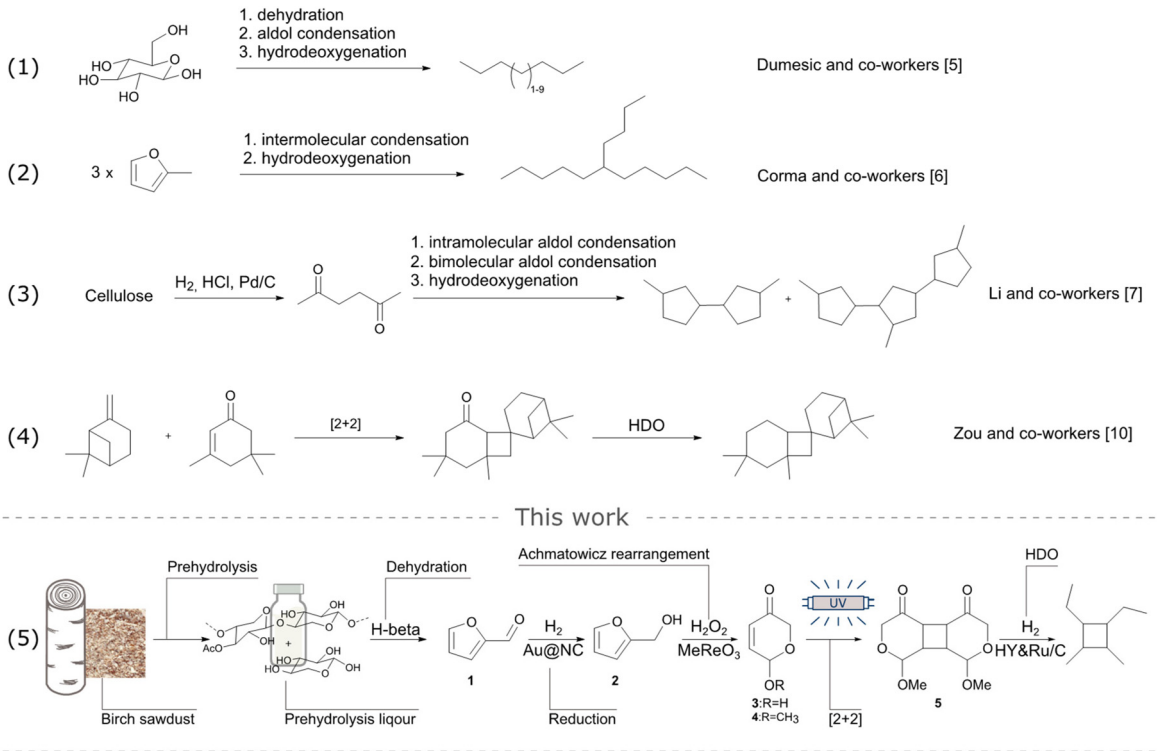

Scheme 1 The state-of-the-art synthesis of liquid hydrocarbons in aviation boiling point range.

pressure mercury lamps (4 W each, maximum irradiation at 365 nm), stirring system, and air circulation. HDO reactions were performed in a stainless-steel reactor assembled from Swagelok units including a gas valve. NMR was performed on a Bruker Avance (400 MHz). Chemical shifts are expressed in parts per million (ppm, δ). GC-MS/FID was performed on a QP2020 system (SHIMADZU, Japan) equipped with two parallel HP-5MS columns (30 m × 0.25 mm × 0.25 μm).

Prehydrolysis

Birch sawdust (0.5 g) and 5 mL of DI water were added to an autoclave and stirred at 200 °C. After 40 min, the reaction was stopped. The suspended residue was filtered off, washed with DI water, and dried at 60 °C overnight. The resulting residue was analysed by two-step hydrolysis to determine carbohydrate and lignin content (ESI†). Prehydrolysis liquor was analysed for monosaccharide content by HPLC (ESI†).

Dehydration

D-(+)-Xylose (75 mg, 0.5 mmol) was dissolved in water (150 μL) in an autoclave. EtOAc (3 mL) was added, followed by H-beta zeolite (25 mg). The reaction was performed at 180 °C for 1 h. After completion, an internal standard (dodecane) was added. The reaction mixture was filtered and subjected to GC-MS/FID analysis. Yield was quantified by GC-FID (ESI†).

Furfural reduction

Synthesis of Au@NC/TiO_2. Gold nanoparticles embedded on N-doped carbon (Au@NC/TiO_2) were prepared by the pyrolysis method reported elsewhere.[13] Typically, $Au(OAc)_3$ (19.0 mg, 0.05 mmol) and 1,10-phenanthroline (18.0 mg, 0.1 mmol, molar ratio Au : ligand = 1 : 2) were stirred in 20 mL of ethanol for approximately 5 min at 60 °C. The TiO_2 support (1.0 g, titanium(IV) oxide, anatase) was then added, and the mixture was stirred for 30 min. After, the solvent was removed using a rotary evaporator. The obtained solid was ground to a fine powder and then pyrolyzed under N_2 atmosphere in an oven (DEKEMA – Austromat 674i) at a heating rate of 20 °C per minute and held at 400 °C for 2 h. The percentage of gold in the fresh catalyst was determined by FAAS as 1.1 wt%.

Hydrogenation of furfural. The hydrogenation method follows the conditions reported elsewhere.[14] Furfural (0.1 mmol), Au@NC/TiO_2 catalyst (20 mg, 2 mol%), and 2 mL of 2-propanol were placed in a 4 mL glass vial (with a septum and glass capillary), which was then placed inside a 75 mL stainless steel reactor filled to 2/3 of its volume with quartz sand. The reactor was connected to the H_2 gas supply and placed in the test unit (Series 5000 Multiple Reactor System, Parr Instrument Co., USA) equipped with a Parr 4843 controller for the setup and control of reaction temperature and magnetic stirring speed. The reactor was purged five times with H_2, leaving the vessel at 30 bar H_2 pressure, and then heated to 100 °C. After the desired time, the reactor was cooled down, depressurized, and the catalyst was removed by centrifugation to recover the crude mixture. The products were analysed by GC-MS. The analyses were performed with Agilent 7890B equipped with a capillary column HP-1 (30 m × 0.25 mm × 0.25 μm) and octadecane was used as an internal standard to determine the conversion and selectivity.

Synthesis of 6-hydroxy-2*H*-pyran-3(6*H*)-one (Achmatowicz rearrangement)

Methyltrioxorhenium (12.5 mg, 50 μmol, 1 mol%) was combined with hydrogen peroxide (855.9 mL, 35%, 5 mmol) and cooled to 0 °C. The mixture was stirred for 15 min. A solution of furfuryl alcohol (490 mg, 5 mmol) in 2-propanol (2.6 mL) was added dropwise to the oxidation solution. The resulting mixture was stirred for 5 h, allowing the temperature to rise to room temperature. Molecular sieves (1.5 g) were then added, and the mixture was left to stir for an additional hour. The reaction mixture was then filtered through a Celite plug, condensed under reduced pressure, and left to crystallize in the freezer overnight. The following morning, the precipitate was filtered off and dried under high vacuum, yielding a colourless crystalline solid (559 mg, 98%).

Synthesis of 6-methoxy-2*H*-pyran-3(6*H*)-one

6-Hydroxy-2*H*-pyran-3(6*H*)-one (790 mg, 6.92 mmol) was dissolved in dry DCM (10 mL). Trimethyl orthoformate (3.78 mL, 34.6 mmol) was added to the solution at 0 °C, followed by the addition of boron trifluoride ($BF_3{\cdot}OEt_2$, 50 μL, 0.41 mmol 5.9 mol%). The reaction was stirred for 1 h at 0° C. Upon completion, additional DCM and saturated $NaHCO_3$ solution were added, and the mixture was extracted three times with DCM. The solvent was removed under reduced pressure. The crude product was purified by flash column chromatography (20% EtOAc : pentane), yielding a colourless oil (608 mg, 69%). Methoxylation was performed to isolate the different stereoisomers of the product and this step was conducted for analysis purposes.

[2 + 2] cycloaddition

The light-driven [2 + 2] cycloaddition was performed in a Rayonet UV reactor. In a quartz tube, 6-methoxy-2*H*-pyran-3(6*H*)-one (154 mg, 1.2 mmol) was dissolved in MeCN (5 mL, 0.24 M). The reaction vessel was placed inside the Rayonet reactor, where the reaction was performed under UV irradiation (365 nm), continuous stirring, and cooling by air circulation. After 48 h, the reaction was stopped and solvent was removed under reduced pressure. The resulting residue was purified by column chromatography (40% EtOAc : pentane), yielding a white crystalline solid (88 mg, 57%). The isolated isomers were characterized by NMR (ESI†), recrystallized and analysed by single-crystal X-ray diffraction (ESI†).

HDO of cycloadducts

The mixture of cycloadduct isomers (100 mg, 0.39 mmol) was loaded into a stainless-steel reactor (25 mL), followed by the addition of solvent (3 mL, 0.13 M). Both catalysts Ru/C (25 mg, 5% Ru content) and HY zeolites (50 mg) were then added. The reactor was sealed and subjected to three cycles of nitrogen

gas flushing through the valve. Following this, hydrogen gas was added to the system. The reaction was conducted in an oil bath maintained at 220 °C for 16 h with continuous stirring. Upon completion, the reactor was cooled down, and the pressure was slowly released. The resulting reaction mixture was filtered to separate solid catalysts, and an aliquot of the filtrate was analysed by GC-MS/FID with dodecane as a standard (ESI†). Due to the complexity of the product mixture, individual components were identified indirectly using GC-MS (ESI†).

Life cycle assessment

To enhance the understanding of environmental impacts related to the extraction and conversion of prehydrolysis liquor into cyclobutane-based aviation fuels, a comparative Life Cycle Assessment (LCA) was conducted. The assessment included two scenarios: S1-Burn depicts the kraft pulping process with an initial prehydrolysis step for extracting hemicellulose, followed by combustion in a co-generation facility to produce heat and electricity; S2-AF considers the conversion of hemicellulose, obtained in the prehydrolysis phase, into cyclobutane-based aviation fuels while the residual hemicellulose is combusted in a co-generation plant to supply heat and electricity.

A consequential LCA approach is adopted as it more effectively captures the environmental implications of decision-making in prehydrolysis liquor management.[15]

A functional unit of 1 kg of unbleached kraft pulp was chosen to focus on the determining product of the system,[16,17] treating all the co-products by substitution. A cradle to gate approach was chosen, thereby excluding the bleaching process, usage phase, and end-of-life of dissolving grade pulp from our analysis. Since these life cycle stages are identical for both scenarios being compared, our chosen approach does not compromise the comparative validity. This assessment is contextualized within Northern Europe, with a subsequent extension to a broader European context examined during the sensitivity analysis. Detailed information on the choices made for scope definition and a comprehensive review of both primary and secondary data sources (Table S8) can be found in ESI.†

The impact assessment results are displayed using 16 midpoint impact categories from the Environmental Footprint (EF) method 3.0.[18] In the main text, only five categories are presented and discussed: climate change (GWP-total), land use (SQP), water use (WDP), resource use of fossils (ADP-fossil), and mineral and metal resources (ADP-min&met). The complete set of indicators and results is available in ESI.†

Aspen Plus

As explained in the previous section, many solvents play a major role in the pathway to prepare cyclobutane-based aviation fuels. According to the principles of the green chemistry, recyclable environmentally benign solvents should be exploited to minimize the burden to eco-systems. In building the inventory phase for the LCA study, an assumption of 2% loss of solvent every 5 runs was assumed and tested through simple simulations with Aspen Plus. The separation of the EtOAc and water mixture from furfural after de-hydration was tested through distillation (Radfrac column) followed by a decanter to separate the EtOAc/water mixture, achieving a loss of EtOAc < 1%. In the same way, 2-propanol and acetonitrile separations from the products were tested through distillation, achieving almost complete separation. These preliminary results confirmed the assumption of small solvent loss and recyclability to minimize the associated environmental impacts.

Results and discussion

Prehydrolysis of birch sawdust

Birch sawdust with hemicellulose (xylan) content of 25% (ESI, Table S1†) was pre-treated using previously reported autogenous hydrolysis conditions.[19] Optimized prehydrolysis (40 min, 200 °C, autogenous pressure) gave 97% removal of hemicelluloses. Only negligible amount of cellulose (0.4 wt% based on the raw material) was solubilized under these conditions. The xylose content in prehydrolysis liquor was measured to be 32% of the initial hemicellulose content (ESI, Table S2†).

Dehydration of xylose

Currently, furfural is industrially produced from C_5 sugars by homogeneous catalysis with mineral acids. The use of mineral acids causes technical challenges such as equipment corrosion and environmental issues.[20] Recent research demonstrated benefits of solid acid catalysis as more environmentally friendly furfural production.[21] Among solid catalysts, inorganic oxides such as zeolites demonstrated their catalytic activity and high selectivity in xylose dehydration into furfural.[22]

Previously we reported a successful transformation of prehydrolysis liquors to furfural using beta zeolites in a dioxane–water mixture as solvent.[19,23] In this work, we explored EtOAc, a more sustainable solvent for the transformation of xylose into furfural.[24]

Dehydration to furfural **1** was performed through catalysis by beta zeolites at 180 °C in EtOAc giving 74% yield under optimized conditions (ESI, Table S3†), slightly lower than using dioxane (83%). It was found that addition of small amounts of water was important for obtaining high yields. Stopping the reaction after 1 h was also crucial to avoid humin formation.

Selective hydrogenation of furfural to furfuryl alcohol

The next step is reduction of furfural **1** to furfuryl alcohol **2**. Selective reduction of the aldehyde moiety in furfural is not trivial due to the competing decarbonylation, hydrogenolysis, and hydrogenation of the furan ring (C=C bonds).[25,26]

Hydrogenation catalysed by Ru/C and Pd/C were tested using 2-propanol as the hydrogen donor (Table 1, entries 1 and 2). Reactions catalysed by Ru/C showed higher conversion of furfural and higher selectivity towards furfuryl alcohol, however, the maximum yield observed was only 53% (Table 1, entry 1).[27] Among the hydrogen donors tested (2-propanol,

Table 1 Furfuryl hydrogenation to furfuryl alcohol

Entry	Cat.	Cat., mol%	Hydrogen source	Conversion of **1**, %	Yield of **2**, %
1	Pd/C	0.5	2-Propanol	90	20
2	Ru/C	0.5	2-Propanol	100	53
3	Ru/C	0.5	H_2 (50 bar)[a]	97	15
4	Au@NC/TiO_2	2.0	H_2 (30 bar)/ 2-propanol	100	99

[a] EtOAc was used as a solvent.

EtOH, MeOH, HCOOH), 2-propanol showed the best performance. When molecular hydrogen was used as a hydrogen source, full conversion was achieved with Ru/C, although selectivity dropped significantly (Table 1, entry 3). Thus, seemingly straight forward reduction proved challenging. Selectivity issues are known in most traditional heterogeneous hydrogenation catalysts, *e.g.*, ruthenium, palladium, and nickel, and we decided to explore a less active metal, such as gold. Gold has been considered catalytically inactive towards H_2, but it can develop into a very selective catalyst once H_2 heterolytic activation occurs across a metal–ligand interface.[28,29] Base ligands, such as ammonia and pyridine, were suggested to be used as additives to improve hydrogenation of aldehydes over gold-based catalysts.[30] DFT calculations suggested that the base allows the chemical adsorption of H_2 and its cleavage *via* an heterolytic dissociation mechanism, forming NH_4^+ and H^- that will be adsorbed on the active metal site. Finally, H^+ (of NH_4^+) and H^- will be transferred to the aldehyde and produce the corresponding alcohol. Later, Rossi and co-workers developed a fully heterogenous gold embedded on N-doped carbon (Au@NC/TiO_2) catalyst, which was active and selective for alkynes semihydrogenation.[13] It was suggested that the heterolytic cleavage of molecular H_2 occur at the basic nitrogen species on the N-doped carbon material in close vicinity of Au nanoparticles. Later, this catalyst was tested for the hydrogenation of various aldehydes to alcohols, showing high selectivity.[14] A similar mechanism was also proposed by Nagpure *et al.*,[31] for hydrogenation of cinnamaldehyde, based on the heterolytic dissociation of H_2, followed by the transfer of nucleophilic H^- ion to electrophilic carbonyl carbon of the aldehyde, whereas the electrophilic H^+ ion transfers to nucleophilic carbonyl oxygen, leading to the desired alcohol.

Gratifyingly, the Au@NC/TiO_2 catalyst showed very high selectivity in the conversion of furfural to furfuryl alcohol, reaching full conversion and no other side-products (Table 1, entry 4). It is worth to mention that the heterogenous catalyst can be recycled and reused, as demonstrated in the hydrogenation of benzaldehyde.[14]

Achmatowicz rearrangement of furfuryl alcohol into compound 3

The classical Achmatowicz rearrangement requires the use of reagents such as *m*-chloroperoxybenzoic acid (*m*-CPBA)[32] or brominating agents (bromine[33] or *N*-bromosuccinmide (NBS)[34]). In these reactions, stoichiometric amounts of waste are generated (Scheme 2), which lowers the sustainability of the rearrangement. More benign approaches have been reported. Examples include, oxidative rearrangement using hydrogen peroxide, catalyzed by homogeneous transition metal complexes such as methyltrioxorhenium (MTO)[35] and vanadyl acetylacetonate ($VO(acac)_2$).[36] Unfortunately, these novel more benign approaches have not been reported for unsubstituted furfuryl alcohol, that is a more challenging substrate.[37,38] Substituted furfuryl alcohols were also needed for the photolytic rearrangement described by Gilmore and co-workers achieved yields up to 89%.[39]

Heterogeneous titanium silicalite (TS-1) has been reported in this transformation.[40] Attempts to use TS-1 catalyst, as previously reported, were unsuccessful. Only 48% yield could be observed, compared to the reported 94%.[40,41] A possible explanation could be the difference in the crystal structure of TS-1 that can significantly influence the activity of the catalyst.[42,43] Even though several different procedures were used to prepare TS-1, higher yields were not achieved, showing challenges with this approach.

We were able to successfully transform unsubstituted furfuryl alcohol into compound **3** *via* epoxidation by hydrogen peroxide using MTO catalyst. MTO together with hydrogen peroxide forms active peroxo-metal species able to catalyse double bond epoxidation.[44] The reaction gave full conversion of the starting material within 5 h (ESI, Table S4†). After 6 h, selectivity towards the product **3** dropped. If the reaction was left for 2 days, the yield of product **3** decreased to 48% (ESI, Table S4†). This is not surprising as product **3** also contain a double bond that can undergo further reactions.

To confirm product degradation, a stability test was performed. After 3 h using standard reaction conditions, half of the product **3** was degraded, and after 12 h, only 28% of the product remained. Therefore, quenching the reaction after 5 h was essential to prevent side-reactions. Attempts to stop the reaction by simple work-up after 5 h were unsuccessful. Perhaps product degradation in the presence of oxidative agents occurred. We proposed to quench the reaction using molecular sieves once the reaction was completed. The reaction and quenching procedure were optimized, and it was shown that 1 h treatment with molecular sieves after 5 h reaction gave 98% isolated yield of compound **3**.

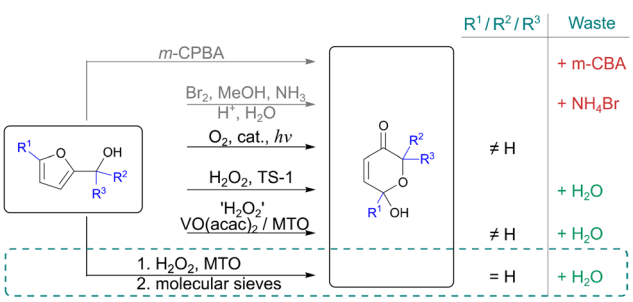

Scheme 2 Achmatowicz rearrangement.

To prevent waste generation at each stage of our transformations, we hypothesized the possibility of recycling the molecular sieves used. When the optimized reaction was completed and quenched, molecular sieves (4 Å) were recovered and dried at 70 °C under reduced pressure for 30 h to release solvent and moisture. Dried molecular sieves were re-used twice, without significant loss in the yield of product **3** (Fig. 2).

Light-driven [2 + 2] cycloaddition

The enone functionality of compound **3** makes it susceptible to light-driven intermolecular [2π + 2π] additions. The self-cycloaddition of enones can occur at longer wavelengths (>300 nm) eliminating the need for a photosensitizer.[45]

In this work, we report, for the first time, the cycloaddition of enone-containing substrate **4** for creating 4-membered adducts (Scheme 2). The resulting adducts are desired precursors for C_{10} cyclobutane-containing aviation fuels.

The substrate **4** was selected for [2 + 2] cycloaddition due to its more convenient handling and the ease of isolating of the isomeric cycloadducts compared to substrate **3**. Compound **4** was synthesised through the methylation of substrate **3** using the procedure described in the Experimental section.

The light absorption spectrum of compound **4** was analysed. In accordance with the anticipated behaviour of the conjugated π-system, the compound showed π–π* absorption band in the range of 300–400 nm, which allows dimerization to occur (ESI, Fig. S1†).

The substrate **4** was irradiated at 365 nm with eight high-pressure mercury lamps (4 W each), resulting in the formation of cycloadducts. The photoreactions were conducted for a total of 48 h, although shorter reaction times can be achieved by employing more powerful lamps. The photoreactions were performed in solution and as neat reactions. The neat reaction gave lower conversion of starting material **4** than the reaction performed in acetonitrile where 79% and 96% conversion, respectively, were observed.

In the concerted light-driven [2 + 2] cycloaddition, the substrate **4** can form two regioisomers: head-to-head (HH) and head-to-tail (HT). Further complexity arises from the possibility of syn- or anti-addition, leading to syn-HH, anti-HH, syn-HT, and anti-HT isomers.[46] In this study, we successfully separated and isolated two anti-HH diastereomers (Scheme 3, cycloadducts 1 and 2, both were racemic mixtures) and one anti-HT isomer (Scheme 3, cycloadduct 3). The structures as well as relative stereoisomers of isolated cycloadduct were confirmed by single-crystal X-ray analysis (ESI, Fig. S2–S4†).

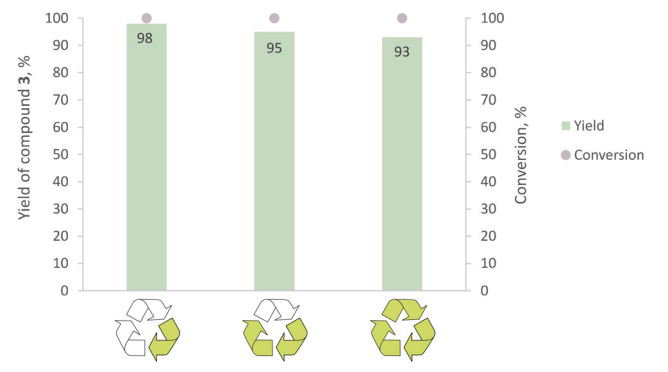

Fig. 2 Recycling of the molecular sieves. Reaction conditions: furfuryl alcohol (10 mmol), 2-propanol, addition at 0 °C, reaction at room temperature, H_2O_2 (1 equiv.), MTO (1 mol%), dried molecular sieves (4 Å) were added after 5 h, the reaction was continued for 1 h more.

Hydrodeoxygenation

As the cycloadducts are highly oxygenated, HDO is required to convert these intermediates to desired aviation fuels.

Before optimizing the HDO conditions for cycloadduct transformation, catalyst screening was performed using substrate **3**. In our initial experiments, we employed Pd/C while running the reaction at 220 °C at 20 bar of hydrogen pressure using cyclohexane as carrier liquid. After 16 h treatment, we observed full conversion of the starting material and the formation of hydroxy-substituted tetrahydropyran (THP-OH) as a major product (Fig. 3). This confirms that Pd/C facilitates hydrogenation, but not full deoxygenation.

When zeolites were introduced together with Pd/C, a shift in the product selectivity towards hydrocarbon formation was observed (Fig. 3). Zeolite screening revealed that the addition of HZSM-5 zeolites (Si/Al ratio of 23) still yielded THP-OH as a major product, while HY zeolites (Si/Al ratio of 30) shifted selectivity towards THP and C_5 hydrocarbons. It is likely that larger channels in HY type of zeolites facilitate better diffusion of the substrates through zeolites, making active sites more accessible. Changing the Si/Al ratio of zeolites from 30 to 80 shifted the selectivity back to THP-OH. This shift is connected to the decreased Brønsted acidity in HY with a Si/Al ratio of 80, compared to a Si/Al of 30.

We then tested other noble metals in tandem with HY zeolites (Si/Al of 30). The performance of Pt/C was similar to Pd/C.

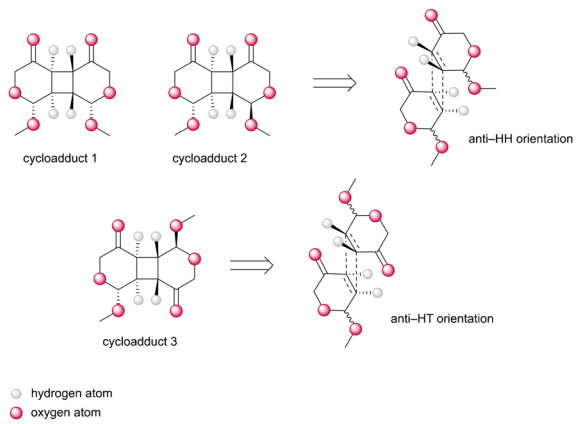

Scheme 3 Isolated cycloadducts. The reaction was performed using the following conditions: In a quartz tube, 6-methoxy-2*H*-pyran-3(6*H*)-one (154 mg, 1.2 mmol) was dissolved in MeCN (5 mL, 0.24 M) and irradiated using UV lamps (365 nm) for 48 h. The cycloadducts were isolated by column chromatography (40% EtOAc : pentane), recrystallized and analysed by single-crystal X-ray diffraction (ESI†).

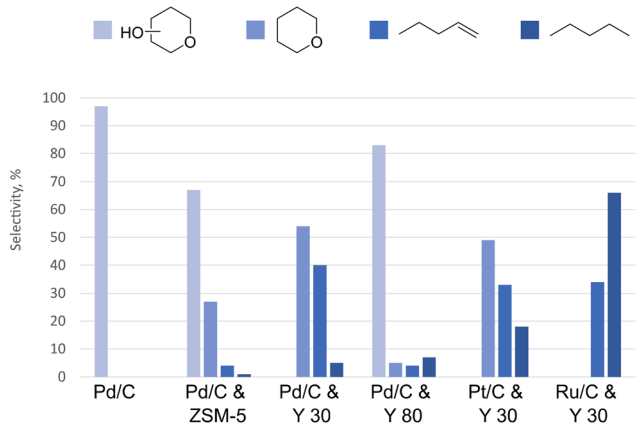

Fig. 3 The distribution of products after hydrotreating the compound **3**. Reaction conditions: compound **3** (0.88 mmol), cyclohexane (3 mL), 220 °C, 20 bar of hydrogen pressure, 16 h.

The more oxophilic Ru/C demonstrated the capacity to hydrodeoxygenate the THP ring, resulting in selective transformation to hydrocarbons (Fig. 3).

With an optimized catalytic system in hand, we performed HDO on the dimeric cycloadducts. The reaction showed full conversion of the starting material and high selectivity towards fully deoxygenated molecules, resulting in a 51% yield of detected hydrocarbons, which included 48% of C_7–C_{10} compounds. Notably, C_9 hydrocarbons were the major product, followed by C_8, suggesting that C–C bond cleavage took place in the form of decarbonylation of reaction intermediates (Table 2, entry 1).[1] Further improvements were attempted by varying carrier liquid (Table 2, entry 2), pressure (Table 2, entries 3 and 4), and reaction temperature (Table 2, entries 5 and 6).

However, no improvement in yields of hydrocarbons in aviation fuel range (C_8–C_{10}) was observed. Increasing the pressure to 80 bar resulted in a shift in selectivity towards C_8 and C_7 products, possibly due to cracking reactions. A similar trend was observed when the temperature was increased to 245 °C. In reactions conducted at lower pressure (Table 2, entry 4) and temperature (Table 2, entry 6), complete deoxygenation was not achieved.

Mass balance

The carbon balance and mass balance were calculated for the proposed value chain. Total carbon yield for the transformation starting from furfural was 48% (Fig. S16, ESI†).

The mass balance of the complete value chain was assessed for two distinct scenarios (Fig. 4). In one scenario (S1-Burn), prehydrolysis liquor, generated during a wood pretreatment step, is utilized as a source of energy through combustion in an external co-generation plant. In the second scenario (S2-AF), the prehydrolysis liquor is utilized to produce furfural with residual side-streams contributing to energy co-generation. Subsequently, furfural undergoes a multi-step transformation process to yield hydrocarbons suitable for aviation fuel applications (S2-AF). Quantitative values, expressed in kilograms, were calculated relative to the functional unit, defined as the kilogram of unbleached pulp.

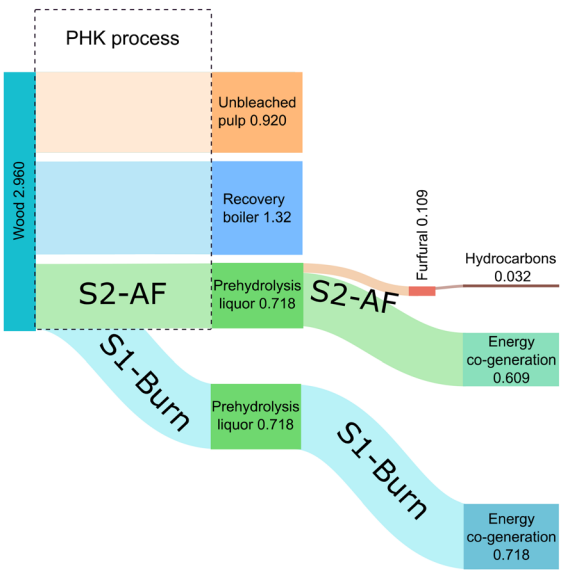

Fig. 4 Mass balance. Values are expressed in kilograms.

Table 2 HDO of cycloadducts catalysed by Ru/C with HY zeolites (Si/Al ratio of 30) at 220 °C and under the hydrogen pressure of 40 bar. Reaction time was 16 h

		Yield, mol%[a]						
Entry	Deviation from the standard condition	$C_{10}H_{20}$	C_9H_{18}	C_8H_{16}	C_7H_{14}	C_8–C_{10} oxygenates	C_5H_{12}	THP
1	—	9	18	14	7	4	3	—
2	Co-solvent (THF)	10	18	14	4	8	—	—
3	80 bar	5	13	19	15	3	9	4
4	20 bar	1	1	4	4	35	5	6
5	245 °C	7	9	17	12	3	7	1
6	195 °C	<1	<1	<1	<1	30	<1	—

[a] Yield determined by GC-FID.

Life cycle assessment

This section presents the findings of the LCA study. A cradle to gate approach was chosen excluding from our scope the bleaching step, the use phase, and the end life of the dissolving grade pulp. These the life cycle phases are equal for both scenarios (*vide supra*) to be compared; thus, this approach won't affect the comparison according to ISO 14044. To model the consumption and production electricity, an average of the marginal electricity of Sweden and Finland was considered, then for heat the substitution of biomass and coal were adopted for Sweden and Finland according to the procedure described by Marson *et al.*

Detailed representations of the process model with the system boundaries are available in ESI (Fig. S6–S9†).

To determine the carbon content [kgC kg^{-1}] in cellulose, hemicellulose and lignin and their Low Heating Value [MJ kg^{-1}] to be used in the model secondary data from Ecoinvent 3.9.1 consequential were exploited. From the values retrieved the theoretical energy that can be produced from incineration phases was calculated and the efficiency of the recovery boiler was calculated to be 13% and used in the modelling of the scenarios. From the same source, secondary data for the values of efficiencies to heat and electricity from a co-generation plant were retrieved and are 45% and 15% respectively.

Fig. 5 graphically illustrates the Life Cycle Impact Assessment outcomes for the primary five categories, with comprehensive data detailed in ESI (Tables S10–S13†). S2-AF emerged as the superior performer in the GWP-total (-5.63×10^{-2} kg CO_2eq $kgUSP^{-1}$) and ADP-min&met categories, while S1-Burn was the most performing in SQP, WDP and ADP-fossil categories.

In GWP-total for S2-AF, the principal factor contributing to reduced impacts was the avoidance of fossil CO_2 emissions relative to conventional aviation fuel, decreasing emissions by 0.57 kg CO_2eq $kgUSP^{-1}$ (USP stands for unbleached sulfate pulp). The efficacy of S1-Burn in the GWP-total, which utilizes prehydrolysis liquor as an energy source in a cogeneration plant, is highly contingent on the replaced energy mix. It should be noted that prehydrolysis liquors are currently burnt in the recovery boiler. When this scenario was calculated, the environmental sustainability was worse in all impact categories; mainly, because the recovery boiler has a lower efficiency. Thus, to study the effect of valorization, incineration in an external co-generation plant was modelled.

Sensitivity analysis reveals that substituting this with a European energy mix enhances environmental benefits, outstripping S2-AF with a GWP-total of −0.634 kg CO_2eq.

Conversely, in the SQP category, S1-Burn outperforms S2-AF, attributable to the increased combustion of hemicellulose for heat production, thereby supplanting biomass-derived heat prevalent in Northern Europe's energy mix. This substitution mitigates wood chip consumption and reduces land use impacts. S2-AF's intensified use of solvents and catalysts leads to greater WDP impacts than S1-Burn.

In terms of ADP-fossil, while biobased aviation fuel production substantially reduces impacts, it does not suffice for an overall benefit in this category due to solvent usage in the value chain upgrade. S1-Burn prevails due to enhanced energy

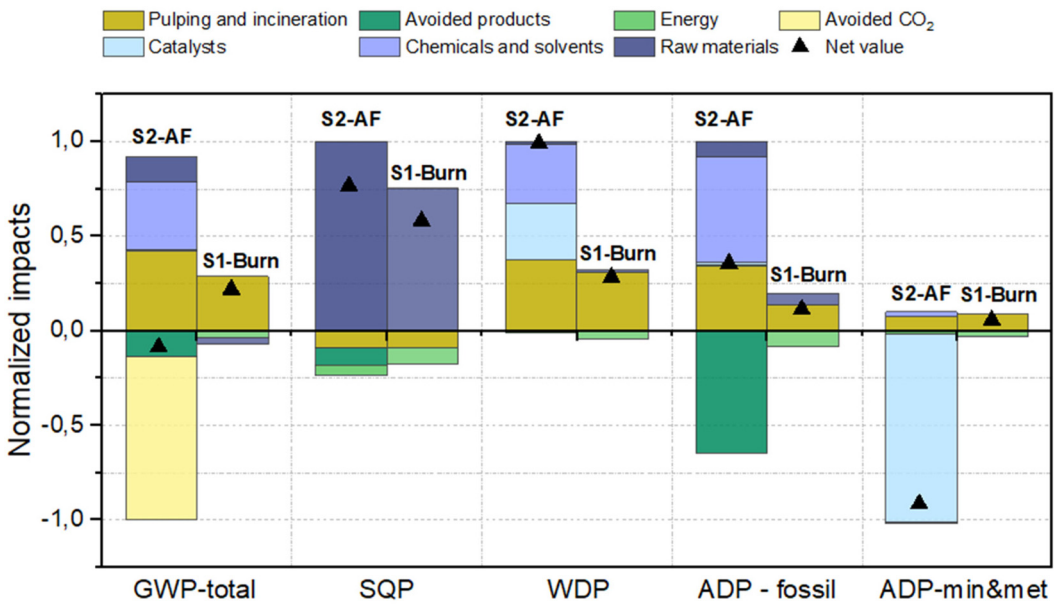

Fig. 5 Contribution of different product system stages comparing S1-Burn and S2-AF. Raw materials: wood chips production. Pulping and incineration: pulping process (including chemicals involved) and all the emissions from the hemicellulose combustion. Chemicals and solvents: chemicals and solvents used in the aviation fuel production chain. Catalysts: catalysts used in the production of aviation fuels. Avoided products: avoided production of pentane and kerosene. Avoided CO_2: avoidance of fossil CO_2 from the combustion of fossil aviation fuels. Energy: Consumption and avoidance (by production from combusted biomass) of energy from the grid.

yield from hemicellulose. For ADP-min&met, S2-AF outstrips S1-Burn since metal extraction for hydrogenation catalyst concurrently yield other metals concurrently yield other metals, diminishing the need for their primary production, as per the Ecoinvent marginal background data. A full discussion of the results in the other impact categories is available in ESI.†

Four sensitivity analyses assessed the effects of various modeling and operational parameters on the outcomes. The most significant involved an average European energy mix scenario for the integrated pulp mill, resulting in notable shifts for both S1-Burn and S2-AF, particularly in GWP-total, WDP, and ADP-fossil. The impact on GWP-total is attributed to the higher emission factor of the European marginal energy mix (0.218 $kgCO_2eq\ kW^{-1}\ h^{-1}$) compared to the Northern mix (0.07 $kgCO_2eq\ kW^{-1}\ h^{-1}$), suggesting a net reduction in greenhouse gas emissions when replacing an energy mix dominated by fossil fuels. A separate sensitivity analysis evaluated the impact of a 10% lower yield to aviation fuels in the hydrodeoxygenation (HDO) section on S2-AF. Although the GWP-total and ADP-fossil indicators deteriorated, as indicated in Table S15,† S2-AF still maintains a climate change advantage over S1-Burn, albeit with increased impacts on fossil resource use.

Another analysis for S2-AF assessed the effects of producing aviation fuels in an isolated facility, predicting increased GWP-total and ADP-fossil due to higher energy demands. However, the results showed a decrease, contrary to expectations, due to varying efficiencies between recovery boilers and co-generation plants in hemicellulose combustion.

Lastly, altering the assessment to the ReCiPe 2016 (midpoint), H method in the final sensitivity analysis did not yield significant differences in the relevant impact categories. ReCiPe 2016 (midpoint) is a Life-Cycle Impact Assessment method which name stands for the initials of the institutes that were the main contributors to the design and development of the method: RIVM and Radboud University, CML, and PRé Consultants. This method calculates 18 midpoint indicators which focus on single environmental issues and express their relative severity.

Conclusions

Prehydrolysis liquors from forestry textile production are generated in kraft mills. As environmental sustainability concerns of cotton production has increased, it has been projected that wood textile production will increase in the future.[47,48] Thus, prehydrolysis liquors will become more available. Currently, these liquors are incinerated in the recovery boiler, which is a bottleneck in pulp mills. This additional load hampers pulp production. This work describes a way to valorize this side-stream beyond its heating value, and at the same time debottleneck pulp production.

Herein, a full value chain from an industrial side-stream to high energy content aviation fuel is demonstrated. The prehydrolysis liquors were transformed to furfural using zeolites. Furfural was reduced using homogeneous catalysis, selectively yielding furfuryl alcohol by transfer hydrogenation. Furfuryl alcohol was then rearranged to the Achmatowicz product using MTO and hydrogen peroxide. The resulting adduct was dimerized using a photo [2 + 2] cycloaddition. HDO of the cycloadducts gave desired hydrocarbons in aviation fuel range. Catalyst screening revealed that Ru/C and zeolites were required to cleave all C–O bonds, including the challenging tetrahydropyran bonds. LCA showed benefits in climate change when implementing this technology in a pulp mill instead of incineration.

This study makes progress in mild and selective HDO of challenging C–O bonds. We hope that this inspires researchers to further development of value chains from available side streams.

Author contributions

Daria Lebedeva conducted investigations and wrote the original draft of the article. Lars William Schick conducted investigations and contributed to the writing process. Withsakorn Sangsuwan conducted investigations. Gonzalo Castiella-Ona participated in the investigation phase. Erik Svensson Grape and A. Ken Inge performed single crystal X-ray analysis to determine the absolute configuration of the [2 + 2] isomers. Dagoberto O. Silva, Liane M. Rossi conducted selective hydrogenation of furfural. Daniel Cracco, Alessandro Marson, and Alessandro Manzardo conducted LCA. Elena Subbotina contributed to the conceptualization of the study. Joseph S. M. Samec provided conceptualization, supervised the research, and contributed to the writing process.

Conflicts of interest

There are no conflicts to declare.

Acknowledgements

JSMS acknowledges Swedish Research Council VR (2020-04143) and Swedish Energy Agency (grant 45903-1). LMR acknowledges King Carl XVI Gustaf 50th Anniversary Fund for Science, Technology and Environment for the King Carl XVI Gustafs professorship in environmental science (Konung Carl XVI Gustafs professur i miljövetenskap).

References

1 J. A. Muldoon and B. G. Harvey, *ChemSusChem*, 2020, **13**, 5777–5807.
2 C. G. Okoye-Chine, K. Otun, N. Shiba, C. Rashama, S. N. Ugwu, H. Onyeaka and C. T. Okeke, *J. CO2 Util.*, 2022, **62**, 102099.

3 A. Singh, S. I. Olsen and P. S. Nigam, *J. Chem. Technol. Biotechnol.*, 2011, **86**, 1349–1353.
4 V. Lundberg, J. Bood, L. Nilsson, E. Axelsson, T. Berntsson and E. Svensson, *Clean Technol. Environ. Policy*, 2014, **16**, 1411–1422.
5 G. W. Huber, J. N. Chheda, C. J. Barrett and J. A. Dumesic, *Science*, 2005, **308**, 1446–1450.
6 A. Corma, O. de la Torre and M. Renz, *Energy Environ. Sci.*, 2012, **5**, 6328–6344.
7 Y. Liu, G. Li, Y. Hu, A. Wang, F. Lu, J.-J. Zou, Y. Cong, N. Li and T. Zhang, *Joule*, 2019, **3**, 1028–1036.
8 T. Dudev and C. Lim, *J. Am. Chem. Soc.*, 1998, **120**, 4450–4458.
9 C. F. Ryan, C. M. Moore, J. H. Leal, T. A. Semelsberger, J. K. Banh, J. Zhu, C. S. McEnally, L. D. Pfefferle and A. D. Sutton, *Sustainable Energy Fuels*, 2020, **4**, 1088–1092.
10 J. Xie, X. Zhang, C. Shi, L. Pan, F. Hou, G. Nie, J. Xie, Q. Liu and J.-J. Zou, *Sustainable Energy Fuels*, 2020, **4**, 911–920.
11 L. Pan, G. Nie, J. Xie, Y. Liu, C. Ma, X. Zhang and J.-J. Zou, *Green Chem.*, 2019, **21**, 5886–5895.
12 D. M. Morris, R. L. Quintana and B. G. Harvey, *ChemSusChem*, 2019, **12**, 1646–1652.
13 J. L. Fiorio, R. V. Gonçalves, E. Teixeira-Neto, M. A. Ortuño, N. López and L. M. Rossi, *ACS Catal.*, 2018, **8**, 3516–3524.
14 R. J. M. Silva, J. L. Fiorio, P. Vidinha and L. M. Rossi, *J. Braz. Chem. Soc.*, 2019, **30**, 2162–2169.
15 T. Schaubroeck, S. Schaubroeck, R. Heijungs, A. Zamagni, M. Brandão and E. Benetto, *Sustainability*, 2021, **13**, 7386.
16 C. Culbertson, T. Treasure, R. Venditti, H. Jameel and R. Gonzalez, *Nord. Pulp Pap. Res. J.*, 2016, **31**, 30–40.
17 A. Marson, J. S. M. Samec and A. Manzardo, *Sci. Total Environ.*, 2023, **882**, 163660.
18 L. Zampori and R. Pant, Suggestions for updating the Product Environmental Footprint (PEF) method, **https://publications.jrc.ec.europa.eu/repository/handle/JRC115959**, (accessed February 9, 2024).
19 D. Lebedeva and J. S. M. Samec, *Sustainable Energy Fuels*, 2023, **7**, 3637–3643.
20 A. S. Mamman, J. Lee, Y. Kim, I. T. Hwang, N. Park, Y. K. Hwang, J. Chang and J. Hwang, *Biofuels, Bioprod. Biorefin.*, 2008, **2**, 438–454.
21 R. Karinen, K. Vilonen and M. Niemelä, *ChemSusChem*, 2011, **4**, 1002–1016.
22 S. B. Kim, S. J. You, Y. T. Kim, S. Lee, H. Lee, K. Park and E. D. Park, *Korean J. Chem. Eng.*, 2011, **28**, 710–716.
23 E. Subbotina, A. Velty, J. S. M. Samec and A. Corma, *ChemSusChem*, 2020, **13**, 4528–4536.
24 C. M. Alder, J. D. Hayler, R. K. Henderson, A. M. Redman, L. Shukla, L. E. Shuster and H. F. Sneddon, *Green Chem.*, 2016, **18**, 3879–3890.
25 H.-Y. Zheng, Y.-L. Zhu, B.-T. Teng, Z.-Q. Bai, C.-H. Zhang, H.-W. Xiang and Y.-W. Li, *J. Mol. Catal. A: Chem.*, 2006, **246**, 18–23.
26 R. Mariscal, P. Maireles-Torres, M. Ojeda, I. Sádaba and M. L. Granados, *Energy Environ. Sci.*, 2016, **9**, 1144–1189.
27 F. Li, W. Zhu, S. Jiang, Y. Wang, H. Song and C. Li, *Int. J. Hydrogen Energy*, 2020, **45**, 1981–1990.
28 J. L. Fiorio, N. López and L. M. Rossi, *ACS Catal.*, 2017, **7**, 2973–2980.
29 D. Ren, L. He, L. Yu, R.-S. Ding, Y.-M. Liu, Y. Cao, H.-Y. He and K.-N. Fan, *J. Am. Chem. Soc.*, 2012, **134**, 17592–17598.
30 I. Cano, A. M. Chapman, A. Urakawa and P. W. N. M. van Leeuwen, *J. Am. Chem. Soc.*, 2014, **136**, 2520–2528.
31 A. S. Nagpure, P. Gogoi and S. V. Chilukuri, *Chem. – Asian J.*, 2021, **16**, 2702–2722.
32 L. Zhu, L. Song and R. Tong, *Org. Lett.*, 2012, **14**, 5892–5895.
33 O. Achmatowicz, P. Bukowski, B. Szechner, Z. Zwierzchowska and A. Zamojski, *Tetrahedron*, 1971, **27**, 1973–1996.
34 E. A. Couladouros and M. P. Georgiadis, *J. Org. Chem.*, 1986, **51**, 2725–2727.
35 J. Finlay, M. A. McKervey and H. Q. N. Gunaratne, *Tetrahedron Lett.*, 1998, **39**, 5651–5654.
36 J. Robertson, C. North and J. E. R. Sadig, *Tetrahedron*, 2011, **67**, 5011–5023.
37 J. Deska, D. Thiel and E. Gianolio, *Synthesis*, 2015, 3435–3450.
38 A. K. Ghosh and M. Brindisi, *RSC Adv.*, 2016, **6**, 111564–111598.
39 M. B. Plutschack, P. H. Seeberger and K. Gilmore, *Org. Lett.*, 2017, **19**, 30–33.
40 S. P. Simeonov, M. A. Ravutsov and M. D. Mihovilovic, *ChemSusChem*, 2019, **12**, 2748–2754.
41 S. P. Simeonov, H. I. Lazarova, M. K. Marinova and M. D. Popova, *Green Chem.*, 2019, **21**, 5657–5664.
42 V. Smeets, E. M. Gaigneaux and D. P. Debecker, *ChemCatChem*, 2022, **14**, e202101132.
43 B. Wang, Y. Guo, J. Zhu, J. Ma and Q. Qin, *Coord. Chem. Rev.*, 2023, **476**, 214931.
44 W. A. Herrmann, R. W. Fischer, W. Scherer and M. U. Rauch, *Angew. Chem., Int. Ed. Engl.*, 1993, **32**, 1157–1160.
45 Y.-J. Chen, H.-L. Wang, N. R. Villarante, G. J. Chuang and C.-C. Liao, *Tetrahedron*, 2013, **69**, 9591–9599.
46 M. Sakamoto, F. Yagishita, M. Kanehiro, Y. Kasashima, T. Mino and T. Fujita, *Org. Lett.*, 2010, **12**, 4435–4437.
47 A. Adler, I. Kumaniaev, A. Karacic, K. R. Baddigam, R. J. Hanes, E. Subbotina, A. W. Bartling, A. J. Huertas-Alonso, A. Moreno, H. Håkansson, A. P. Mathew, G. T. Beckham and J. S. M. Samec, *Joule*, 2022, **6**, 1845–1858.
48 K. Witthayolankowit, A. Marson, K. R. Baddigam, D. Lebedeva, M. Shaikh, A. Kane, D. Gupta, M. I. Wide, A. P. Mathew, D. Kubička, A. Manzardo and J. S. M. Samec, *Chem. Eng. J.*, 2023, **470**, 144179.